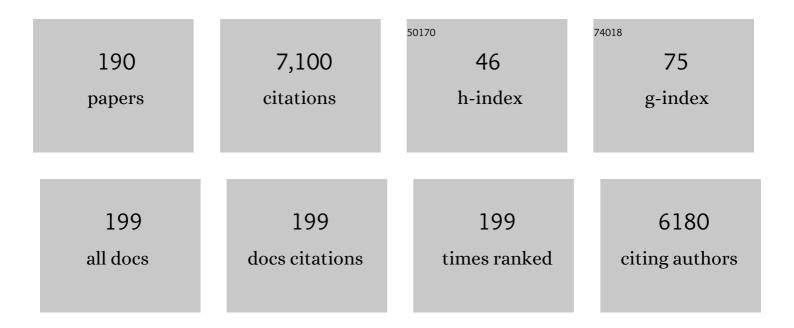
## Michael J Hoffmann

List of Publications by Year in descending order

Source: https://exaly.com/author-pdf/3575384/publications.pdf Version: 2024-02-01



#	Article	IF	CITATIONS
1	Upscaling of LATP synthesis: Stoichiometric screening of phase purity and microstructure to ionic conductivity maps. Ionics, 2021, 27, 2017-2025.	1.2	10
2	Evolution of ferroelectric domains in methylammonium lead iodide and correlation with the performance of perovskite solar cells. Journal of Materials Chemistry A, 2021, 9, 21845-21858.	5.2	7
3	Uncovering the symmetry of the induced ferroelectric phase transformation in polycrystalline barium titanate. Journal of Applied Physics, 2021, 130, .	1.1	9
4	Ferroelectric Poling of Methylammonium Lead Iodide Thin Films. Advanced Functional Materials, 2020, 30, 1908657.	7.8	36
5	The mechanism of grain growth at general grain boundaries in SrTiO3. Scripta Materialia, 2020, 188, 206-211.	2.6	13
6	Grain size effects in donor doped lead zirconate titanate ceramics. Journal of Applied Physics, 2020, 128, .	1.1	25
7	Interpreting rheology and electrical conductivity: It all boils down to which particle size. Journal of Colloid and Interface Science, 2020, 574, 97-109.	5.0	3
8	Fabrication and Characterization of Fully Inkjet Printed Capacitors Based on Ceramic/Polymer Composite Dielectrics on Flexible Substrates. Scientific Reports, 2019, 9, 13324.	1.6	27
9	Development and characterization of half-cells based on thin solid state ionic conductors for Li-ion batteries. Solid State Ionics, 2019, 333, 66-71.	1.3	3
10	Non-Arrhenius grain growth in strontium titanate: Quantification of bimodal grain growth. Acta Materialia, 2019, 174, 105-115.	3.8	14
11	Internal load transfer in an interpenetrating metal/ceramic composite material studied using energy dispersive synchrotron X-ray diffraction. Materials Science & Engineering A: Structural Materials: Properties, Microstructure and Processing, 2019, 753, 247-252.	2.6	21
12	Influence of PbO stoichiometry on the properties of PZT ceramics and multilayer actuators. Journal of the American Ceramic Society, 2019, 102, 5401-5414.	1.9	11
13	Effect of drilling-induced damage on the open hole flexural fatigue of carbon/epoxy composites. Composite Structures, 2019, 215, 238-248.	3.1	27
14	Ferroelectric Properties of Perovskite Thin Films and Their Implications for Solar Energy Conversion. Advanced Materials, 2019, 31, e1806661.	11.1	89
15	Powder Injection Molding of Oxide Ceramic CMC. Key Engineering Materials, 2019, 809, 148-152.	0.4	4
16	On the ferroelectricity of CH3NH3PbI3 perovskites. Nature Materials, 2019, 18, 1050-1050.	13.3	30
17	Characterization of grain boundary disconnections in SrTiO3 Part II: the influence of superimposed disconnections on image analysis. Journal of Materials Science, 2019, 54, 3710-3725.	1.7	12
18	Processing and characterization of elastic and thermal expansion behaviour of interpenetrating Al12Si/alumina composites. Materials Science & Engineering A: Structural Materials: Properties, Microstructure and Processing, 2019, 743, 339-348.	2.6	36

#	Article	IF	CITATIONS
19	Characterization of grain boundary disconnections in SrTiO3 part I: the dislocation component of grain boundary disconnections. Journal of Materials Science, 2019, 54, 3694-3709.	1.7	18
20	Grain growth in strontium titanate in electric fields: The impact of spaceâ€charge on the grainâ€boundary mobility. Journal of the American Ceramic Society, 2019, 102, 3779-3790.	1.9	34
21	Probing the Microstructure of Methylammonium Lead Iodide Perovskite Solar Cells. Energy Technology, 2019, 7, 1800989.	1.8	29
22	The role of point defects and defect gradients in flash sintering of perovskite oxides. Acta Materialia, 2019, 165, 398-408.	3.8	65
23	Anti-thermal grain growth in SrTiO3: Coupled reduction of the grain boundary energy and grain growth rate constant. Acta Materialia, 2018, 149, 11-18.	3.8	23
24	On the importance of ferroelectric domains for the performance of perovskite solar cells. Nano Energy, 2018, 48, 20-26.	8.2	52
25	Effect of damage by hydroxyl generation on strength of silica fibers. Journal of the American Ceramic Society, 2018, 101, 2724-2726.	1.9	8
26	Diffusion of water in silica: Influence of moderate stresses. Journal of the American Ceramic Society, 2018, 101, 1180-1190.	1.9	8
27	Biaxial strength and slow crack growth in porous alumina with silica sintering aid. Journal of the European Ceramic Society, 2018, 38, 665-670.	2.8	6
28	Tape casted thin films of solid electrolyte Lithium-Lanthanum-Titanate. Solid State Ionics, 2018, 328, 25-29.	1.3	11
29	Reduction of the Sintering Temperature for the Manufacturing of Carbonâ€Rich Dense SiOC Bulk Ceramics. Advanced Engineering Materials, 2018, 20, 1800369.	1.6	3
30	Control of the Surface Morphology of Ceramic/Polymer Composite Inks for Inkjet Printing. Advanced Engineering Materials, 2018, 20, 1800318.	1.6	7
31	Probing the Microstructure of Methylammonium Lead Iodide Solar Cells. , 2018, , .		0
32	A comparison of power controlled flash sintering and conventional sintering of strontium titanate. Scripta Materialia, 2017, 130, 187-190.	2.6	31
33	Double layer electrical conductivity as a stability criterion for concentrated colloidal suspensions. Colloids and Surfaces A: Physicochemical and Engineering Aspects, 2017, 520, 9-16.	2.3	10
34	Ferroelectric domains in methylammonium lead iodide perovskite thin-films. Energy and Environmental Science, 2017, 10, 950-955.	15.6	178
35	Diffusion of water in silica glass in the absence of stresses. Journal of the American Ceramic Society, 2017, 100, 3895-3902.	1.9	7
36	Identification of residual stress layers at glass surfaces via crack terminating angles. Journal of the American Ceramic Society, 2017, 100, 4173-4179.	1.9	1

#	Article	IF	CITATIONS
37	The equilibrium crystal shape of strontium titanate: Impact of donor doping. Scripta Materialia, 2017, 127, 118-121.	2.6	10
38	Stressâ€Enhanced Swelling of Silica: Effect on Strength. Journal of the American Ceramic Society, 2016, 99, 2956-2963.	1.9	9
39	Sintering and grain growth in SrTiO <sub>3</sub> : impact of defects on kinetics. Journal of the Ceramic Society of Japan, 2016, 124, 346-353.	0.5	29
40	Precursor derived SiOC/MoSi <sub>2</sub> -composites for diesel glow plugs: preparation and high temperature properties. Journal of the Ceramic Society of Japan, 2016, 124, 1017-1022.	0.5	4
41	Phase-field study of pore-grain boundary interaction. Journal of the Ceramic Society of Japan, 2016, 124, 329-339.	0.5	20
42	Grain growth in weak electric fields in strontium titanate: Grain growth acceleration by defect redistribution. Journal of the European Ceramic Society, 2016, 36, 2773-2780.	2.8	34
43	Grain growth in perovskites: What is the impact of boundary transitions?. Current Opinion in Solid State and Materials Science, 2016, 20, 286-298.	5.6	41
44	Evolution of microstructure and its relation to ionic conductivity in Li1+xAlxTi2â^'x(PO4)3. Solid State Ionics, 2016, 288, 235-239.	1.3	68
45	Lithium Diffusion Pathway in Li <sub>1.3</sub> Al <sub>0.3</sub> Ti <sub>1.7</sub> (PO <sub>4</sub> ) <sub>3</sub> (LATP) Superionic Conductor. Inorganic Chemistry, 2016, 55, 2941-2945.	1.9	188
46	Grain growth transitions of perovskite ceramics and their relationship to abnormal grain growth and bimodal microstructures. Journal of Materials Science, 2016, 51, 1756-1765.	1.7	36
47	The mechanism of grain boundary motion in SrTiO3. Journal of Materials Science, 2016, 51, 467-475.	1.7	33
48	Growth of single crystalline seeds into polycrystalline strontium titanate: Anisotropy of the mobility, intrinsic drag effects and kinetic shape of grain boundaries. Acta Materialia, 2015, 95, 111-123.	3.8	41
49	Mechanisms of aging and fatigue in ferroelectrics. Materials Science and Engineering B: Solid-State Materials for Advanced Technology, 2015, 192, 52-82.	1.7	278
50	Sol-Gel Processing and Electrochemical Conversion of Inverse Spinel-Type Li2NiF4. Journal of the Electrochemical Society, 2015, 162, A679-A686.	1.3	11
51	Non-Arrhenius behavior of grain growth in strontium titanate: New evidence for a structural transition of grain boundaries. Scripta Materialia, 2015, 101, 68-71.	2.6	67
52	Direct synthesis of trirutile-type LiMgFeF6 and its electrochemical characterization as positive electrode in lithium-ion batteries. Journal of Power Sources, 2015, 274, 1200-1207.	4.0	11
53	Anti-thermal behavior of materials. Scripta Materialia, 2015, 103, 1-5.	2.6	26
54	Volume Expansion Caused by Water Penetration into Silica Glass. Journal of the American Ceramic Society, 2015, 98, 78-87.	1.9	47

#	Article	IF	CITATIONS
55	Chemical and structural effects on the high-temperature mechanical behavior of (1â^' <i>x</i> )(Na1/2Bi1/2)TiO3- <i>x</i> BaTiO3 ceramics. Journal of Applied Physics, 2015, 117, .	1.1	27
56	A reversible wetting transition in strontium titanate and its influence on grain growth and the grain boundary mobility. Acta Materialia, 2015, 101, 80-89.	3.8	19
57	The Impact of Heat Treatment on the Domain Configuration and Strain Behavior in Pb[Zr,Ti]O <sub>3</sub> Ferroelectrics. Journal of the American Ceramic Society, 2015, 98, 269-277.	1.9	5
58	The equilibrium crystal shape of strontium titanate and its relationship to the grain boundary plane distribution. Acta Materialia, 2015, 82, 32-40.	3.8	54
59	Fatigue Threshold <i>R</i> â€curves Predict Fatigue Endurance Strength for Selfâ€Reinforced Silicon Nitride. Journal of the American Ceramic Society, 2014, 97, 577-583.	1.9	4
60	A Novel Approach for the Processing of Advanced Polymer Derived Ceramics with Carbon Nanotubes with the Help of Pores. Advanced Engineering Materials, 2014, 16, 295-300.	1.6	5
61	Bimodal domain configuration and wedge formation in tetragonal Pb[Zr1â^'xTix]O3 ferroelectrics. Computational Materials Science, 2014, 81, 123-132.	1.4	9
62	Phaseâ€ <scp>F</scp> ield Modeling of Diffusion Coupled Crack Propagation Processes. Advanced Engineering Materials, 2014, 16, 142-146.	1.6	14
63	Microstructure of sodium-potassium niobate ceramics sintered under high alkaline vapor pressure atmosphere. Journal of the European Ceramic Society, 2014, 34, 4213-4221.	2.8	28
64	Numerical Determination of the Effective Magnetic Path Length of a Single-Sheet Tester. IEEE Transactions on Magnetics, 2014, 50, 929-932.	1.2	16
65	Influence of temperature and upper cut-off voltage on the formation of lithium-ion cells. Journal of Power Sources, 2014, 264, 100-107.	4.0	39
66	Water Penetration—Its Effect on the Strength and Toughness of Silica Glass. Metallurgical and Materials Transactions A: Physical Metallurgy and Materials Science, 2013, 44, 1164-1174.	1.1	39
67	A micromechanically motivated finite element approach to the fracture toughness of silicon nitride. Journal of the European Ceramic Society, 2013, 33, 1729-1736.	2.8	11
68	Sintering and microstructure of potassium niobate ceramics with stoichiometric composition and with potassium- or niobium excess. Journal of the European Ceramic Society, 2013, 33, 2127-2139.	2.8	12
69	Heat treatment effects on domain configuration and strain under electric field in undoped Pb[Zr <inf>x</inf> Ti <inf>1−x</inf> ]O <inf>3</inf> ferroelectrics. , 2013, , .		0
70	The effect of water penetration on crack growth in silica glass. Engineering Fracture Mechanics, 2013, 100, 3-16.	2.0	32
71	Fatigue Crack Growth Behavior of Silicon Nitride: Roles of Grain Aspect Ratio and Intergranular Film Composition. Journal of the American Ceramic Society, 2013, 96, 259-265.	1.9	15
72	Interactions of defect complexes and domain walls in CuO-doped ferroelectric (K,Na)NbO3. Applied Physics Letters, 2013, 102, .	1.5	62

#	Article	IF	CITATIONS
73	Characterization of Elastic Properties in Porous Silicon Carbide Preforms Fabricated Using Polymer Waxes as Pore Formers. Journal of the American Ceramic Society, 2013, 96, 2269-2275.	1.9	15
74	Influence of the A/B Stoichiometry on Defect Structure, Sintering, and Microstructure in Undoped and Cu-Doped KNN. , 2012, , 209-251.		2
75	Critical mechanical and electrical transition behavior of BaTiO3: The observation of mechanical double loop behavior. Journal of Applied Physics, 2012, 112, .	1.1	25
76	High capacity vertical aligned carbon nanotube/sulfur composite cathodes for lithium–sulfur batteries. Chemical Communications, 2012, 48, 4097.	2.2	282
77	Effect of Water on the Inert Strength of Silica Glass: Role of Water Penetration. Journal of the American Ceramic Society, 2012, 95, 3847-3853.	1.9	21
78	Influence of the A/B nonstoichiometry, composition modifiers, and preparation methods on properties of Li- and Ta-modified (K,Na)NbO3 ceramics. Journal of Applied Physics, 2012, 112, .	1.1	7
79	Universal Polarization Switching Behavior of Disordered Ferroelectrics. Advanced Functional Materials, 2012, 22, 2058-2066.	7.8	82
80	Fabrication and High Temperature Creep Behaviour of Interpenetrated Nickel–Chromium/Alumina Composites. Advanced Engineering Materials, 2012, 14, 795-801.	1.6	2
81	A Residual Stress Intensity Factor Solution for Knoop Indentation Cracks. International Journal of Fracture, 2012, 175, 65-71.	1.1	3
82	Processing and Properties of Coâ€Extruded Lead Zirconate Titanate Fibers. Journal of the American Ceramic Society, 2012, 95, 108-116.	1.9	6
83	The Role of Binder Adsorption for High Solid Loading Nanoâ€Zirconia Extrusion Pastes. Journal of the American Ceramic Society, 2012, 95, 1901-1910.	1.9	0
84	Processing and Elastic Property Characterization of Porous <scp><scp>SiC</scp></scp> Preform for Interpenetrating Metal/Ceramic Composites. Journal of the American Ceramic Society, 2012, 95, 3078-3083.	1.9	29
85	<i>In situ</i> neutron diffraction study of electric field induced structural transitions in lanthanum doped lead zirconate titanate. Zeitschrift Für Kristallographie, 2011, 226, 155-162.	1.1	14
86	An Overview of the Structure and Properties of Siliconâ€Based Oxynitride Glasses. International Journal of Applied Glass Science, 2011, 2, 63-83.	1.0	64
87	Electric Field-Assisted Sintering in Comparison with the Hot Pressing of Yttria-Stabilized Zirconia. Journal of the American Ceramic Society, 2011, 94, 24-31.	1.9	58
88	Crack-Tip Toughness from Vickers Crack-Tip Opening Displacements for Materials with Strongly Rising R-Curves. Journal of the American Ceramic Society, 2011, 94, 1884-1892.	1.9	18
89	Electric Field-Assisted Sintering and Hot Pressing of Semiconductive Zinc Oxide: A Comparative Study. Journal of the American Ceramic Society, 2011, 94, 2344-2353.	1.9	33
90	Effect of Water Penetration on the Strength and Toughness of Silica Glass. Journal of the American Ceramic Society, 2011, 94, s196.	1.9	46

#	Article	IF	CITATIONS
91	Interaction of Modified ( <scp>K</scp> , <scp>Na</scp> NbO <sub>3</sub> Ceramics with <scp>Ag</scp> â€Containing Electrodes. Journal of the American Ceramic Society, 2011, 94, 3591-3595.	1.9	13
92	Sinter-HIP of polymer-derived Al2O3–SiC composites with high SiC contents. Materials Letters, 2011, 65, 2462-2465.	1.3	11
93	CuO-doped NaNOO		

#	Article	IF	CITATIONS
109	Influence of Sr/Ti Stoichiometry on the Densification Behavior of Strontium Titanate. Journal of the American Ceramic Society, 2009, 92, 601-606.	1.9	52
110	Lead Zirconate Titanate–Magnetoplumbite Composites: A First Step Toward Multiferroic Ceramics?. Journal of the American Ceramic Society, 2009, 92, 2362-2367.	1.9	3
111	Influence of crystal structure on crack propagation under cyclic electric loading in lead–zirconate–titanate. Journal of the European Ceramic Society, 2009, 29, 425-430.	2.8	8
112	Development of a roadmap for advanced ceramics: 2010–2025. Journal of the European Ceramic Society, 2009, 29, 1549-1560.	2.8	123
113	Direct comparison between hot pressing and electric field-assisted sintering of submicron alumina. Acta Materialia, 2009, 57, 5454-5465.	3.8	154
114	Local variations in defect polarization and covalent bonding in ferroelectric Cu2+-doped PZT and KNN functional ceramics at the morphotropic phase boundary. Physical Chemistry Chemical Physics, 2009, 11, 8698.	1.3	62
115	Formation of magnetic grains in ferroelectric Pb[Zr0.6Ti0.4]O3 ceramics doped with Fe3+ above the solubility limit. Applied Physics Letters, 2009, 94, 142901.	1.5	41
116	Defect structure and formation of defect complexes in Cu2+-modified metal oxides derived from a spin-Hamiltonian parameter analysis. Molecular Physics, 2009, 107, 1981-1986.	0.8	37
117	Different R-Curves for Two- and Three-Dimensional Cracks. International Journal of Fracture, 2008, 153, 153-159.	1.1	14
118	Mode-II shielding-curve of Al2O3 from measurement of cone crack angles. Journal of Materials Science, 2008, 43, 2077-2081.	1.7	0
119	Method for the estimation of the total displacement of ferroelectric actuators under mixed thermal and electrical loading. Sensors and Actuators A: Physical, 2008, 144, 328-336.	2.0	14
120	DEFECT STRUCTURE IN "SOFT" ( <font>Gd</font> , <font>Fe</font> )-CODOPED PZT 52.5/47.5 PIEZOELECTRIC CERAMICS. Functional Materials Letters, 2008, 01, 7-11.	0.7	15
121	Development of Dense Fillerâ€Free Polymerâ€Derived SiOC Ceramics by Fieldâ€Assisted Sintering. Journal of the American Ceramic Society, 2008, 91, 3803-3805.	1.9	70
122	<i>R</i> urve Determination for the Initial Stage of Crack Extension in Si <sub>3</sub> N <sub>4</sub> . Journal of the American Ceramic Society, 2008, 91, 3638-3642.	1.9	31
123	Characterization of (Fe <sub>Zr,Ti</sub> -V <sub>o</sub> <sup>ldrldr</sup> ) <sup>ldr</sup> defect dipoles in (La,Fe)-codoped PZT 52.5/47.5 piezoelectric ceramics by multifrequency electron paramagnetic resonance spectroscopy. IEEE Transactions on Ultrasonics, Ferroelectrics, and Frequency Control. 2008. 55. 1061-1068.	1.7	37
124	Effects of temperature on poling behavior and high field strain of morphotropic PZT. , 2008, , .		0
125	Defect-Dipole Formation in Copper-Doped <mml:math xmlns:mml="http://www.w3.org/1998/Math/MathML" display="inline"&gt;<mml:msub><mml:mi>PbTiO</mml:mi><mml:mn>3</mml:mn></mml:msub>Ferro Physical Review Letters. 2008. 100. 095504.</mml:math 	electrics.	118
126	Determination of <i>v</i> – <i>K</i> curves from lifetime tests with reloaded survivals. International Journal of Materials Research, 2008, 99, 1107-1112.	0.1	1

#	Article	IF	CITATIONS
127	Characterization of ferroelectric domains in morphotropic potassium sodium niobate with scanning probe microscopy. Applied Physics Letters, 2007, 90, 252905.	1.5	66
128	Nonlinearity of strain and strain hysteresis in morphotropic LaSr-doped lead zirconate titanate under unipolar cycling with high electric fields. Journal of Applied Physics, 2007, 101, 044101.	1.1	67
129	xmlns:mml="http://www.w3.org/1998/Math/MathML" display="inline"> <mml:mrow><mml:mi mathvariant="normal"&gt;Pb<mml:mrow><mml:mo>[</mml:mo><mml:msub><mml:mi mathvariant="normal"&gt;Zr<mml:mrow><mml:mn>1</mml:mn><mml:mo>â^`</mml:mo>xmathvariant="normal"&gt;Ti<mml:mi>x</mml:mi></mml:mrow></mml:mi </mml:msub><mml:mo>]</mml:mo></mml:mrow><m< td=""><td>nml:mi&gt;<!--</td--><td>mml:mrow&gt;&lt;</td></td></m<></mml:mi </mml:mrow>	nml:mi> </td <td>mml:mrow&gt;&lt;</td>	mml:mrow><
130	Declever of the second se	1.2	30
131	Nanodomain structure ofPb[Zr1â^xTix]O3at its morphotropic phase boundary: Investigations from local to average structure. Physical Review B, 2007, 75, .	1.1	264
132	Composition dependence of the domain configuration and size in Pb(Zr1â^'xTix)O3 ceramics. Journal of Applied Physics, 2007, 101, 074107.	1.1	93
133	Nanodomains in morphotropic lead zirconate titanate ceramics: On the origin of the strong piezoelectric effect. Journal of Applied Physics, 2007, 102, .	1.1	128
134	Estimation of strain from piezoelectric effect and domain switching in morphotropic PZT by combined analysis of macroscopic strain measurements and synchrotron X-ray data. Acta Materialia, 2007, 55, 1849-1861.	3.8	107
135	Temperature dependence of poling strain and strain under high electric fields in LaSr-doped morphotropic PZT and its relation to changes in structural characteristics. Acta Materialia, 2007, 55, 5780-5791.	3.8	96
136	Low temperature sintering and high piezoelectric properties of strontium doped PNZT–PNN ceramics processed via the columbite route. Journal of the European Ceramic Society, 2007, 27, 3613-3617.	2.8	9
137	Bipolar Fatigue Caused by Field Screening in Pb(Zr,Ti)O3Ceramics. Journal of the American Ceramic Society, 2007, 90, 070922001254005-???.	1.9	36
138	Permittivity and loss tangent of unpoled LaSr-doped PZT under compressive loading. Journal of Materials Science, 2007, 42, 8753-8756.	1.7	2
139	Iron-oxygen vacancy defect association in polycrystalline iron-modifiedPbZrO3antiferroelectrics: Multifrequency electron paramagnetic resonance and Newman superposition model analysis. Physical Review B, 2006, 73, .	1.1	48
140	Multifrequency electron paramagnetic resonance analysis of polycrystalline gadolinium-doped PbTiO3—Charge compensation and site of incorporation. Applied Physics Letters, 2006, 88, 122506.	1.5	36
141	Measuring Electrostatic Potential Profiles across Amorphous Intergranular Films by Electron Diffraction. Microscopy and Microanalysis, 2006, 12, 160-169.	0.2	4
142	Experimental evidence of the impact of rare-earth elements on particle growth and mechanical behaviour of silicon nitride. Materials Science & Engineering A: Structural Materials: Properties, Microstructure and Processing, 2006, 422, 66-76.	2.6	84
143	Effect of intergranular glass on phase relation of Nd-α-sialon. Scripta Materialia, 2006, 54, 1469-1473.	2.6	4
144	Influence of the Rare-Earth Element on the Mechanical Properties of RE-Mg-Bearing Silicon Nitride. Journal of the American Ceramic Society, 2005, 88, 2485-2490.	1.9	89

#	Article	IF	CITATIONS
145	High-field/high-frequency EPR of paramagnetic functional centers in Cu2+- and Fe3+-modified polycrystalline Pb[ZrxTi1â^'x]O3 ferroelectrics. Magnetic Resonance in Chemistry, 2005, 43, S166-S173.	1.1	41
146	Electrical conductivity and stability of concentrated aqueous alumina suspensions. Journal of Colloid and Interface Science, 2005, 286, 579-588.	5.0	80
147	Structural Analysis of Ceramic Suspensions by CRYO-SEM Investigations. , 2005, , 41-46.		Ο
148	Experimental measurement of stress at a four-domain junction in lead zirconate titanate. Journal of Applied Physics, 2005, 97, 094102.	1.1	30
149	Three-dimensional organization of rare-earth atoms at grain boundaries in silicon nitride. Applied Physics Letters, 2005, 87, 061911.	1.5	62
150	Determination of Stability Areas of Yb- and Nd-α-SiAlON Phases Using the Rietveld Method. Key Engineering Materials, 2004, 264-268, 1075-1078.	0.4	2
151	Impact of the Intergranular Film Properties on Microstructure and Mechanical Behavior of Silicon Nitride. Key Engineering Materials, 2004, 264-268, 775-780.	0.4	18
152	Influence of Grain Size on the Tensile Creep Behavior of Ytterbiumâ€Containing Silicon Nitride. Journal of the American Ceramic Society, 2004, 87, 421-430.	1.9	8
153	Microstructural development of Y- $\hat{l}$ ±/( $\hat{l}^2$ )-sialons after post heat-treatment and its effect on mechanical properties. Ceramics International, 2004, 30, 229-238.	2.3	8
154	Determination of functional center local environment in copper-modified Pb[Zr0.54Ti0.46]O3 ceramics. Journal of Applied Physics, 2004, 95, 8092-8096.	1.1	28
155	High strain lead-based perovskite ferroelectrics. Current Opinion in Solid State and Materials Science, 2004, 8, 51-57.	5.6	57
156	The influence of Mg substitution for Al on the properties of SiMeRE oxynitride glasses. Journal of Non-Crystalline Solids, 2004, 333, 124-128.	1.5	37
157	Structure and rheological properties of the RE–Si–Mg–O–N (RE=Sc, Y, La, Nd, Sm, Gd, Yb and Lu) glasses. Journal of Non-Crystalline Solids, 2004, 344, 8-16.	1.5	58
158	Devising a method of making actuators with reduced poling-induced tension. Sensors and Actuators A: Physical, 2003, 107, 14-20.	2.0	3
159	Effect of the Amount of Additives and Postâ€Heat Treatment on the Microstructure and Mechanical Properties of Yttrium–α‧ialon Ceramics. Journal of the American Ceramic Society, 2003, 86, 2136-2142.	1.9	38
160	Phase Relationships in Neodymia and Ytterbia Containing SiAlONs. Key Engineering Materials, 2003, 237, 43-48.	0.4	8
161	Processing and Microstructural Evolution of Rare Earth Containing SiAlONs. Key Engineering Materials, 2003, 237, 141-148.	0.4	15
162	Influence of Grade of Agglomeration and Green Body Liquid Saturation on Bending Strength and Fracture Toughness of Slip-Cast Alumina. Key Engineering Materials, 2002, 206-213, 641-644.	0.4	2

#	Article	IF	CITATIONS
163	Solubility of Si <sub>3</sub> N <sub>4</sub> in Liquid SiO <sub>2</sub> . Journal of the American Ceramic Society, 2002, 85, 25-32.	1.9	36
164	Analysis of intrinsic lattice deformation in PZT-ceramics of different compositions. Journal of the European Ceramic Society, 2001, 21, 1349-1352.	2.8	43
165	Contribution from Ferroelastic Domain Switching Detected Using Xâ€ray Diffraction to <i>R</i> urves in Lead Zirconate Titanate Ceramics. Journal of the American Ceramic Society, 2001, 84, 2921-2929.	1.9	34
166	Longâ€Term Behavior and Application Limits of Plasmaâ€Sprayed Zirconia Thermal Barrier Coatings. Journal of the American Ceramic Society, 2001, 84, 1301-1308.	1.9	42
167	SiC-Ceramics with Tailored Porosity Gradients for Combustion Chambers. Key Engineering Materials, 2000, 175-176, 149-162.	0.4	16
168	Hard and Tough α-SiAION Ceramics. Materials Science Forum, 2000, 325-326, 219-224.	0.3	9
169	Substitution of Y2O3 by a rare earth oxide mixture as sintering additive of Si3N4 ceramics. Materials Letters, 2000, 45, 39-42.	1.3	44
170	Preparation of Multiple ation alpha‣iAlON Ceramics Containing Lanthanum. Journal of the American Ceramic Society, 1999, 82, 229-232.	1.9	31
171	Preparation of βâ€Silicon Nitride Seeds for Selfâ€Reinforced Silicon Nitride Ceramics. Journal of the American Ceramic Society, 1999, 82, 1608-1610.	1.9	26
172	Title is missing!. , 1998, 2, 75-84.		34
173	Sintering Model for Mixedâ€Oxideâ€Derived Lead Zirconate Titanate Ceramics. Journal of the American Ceramic Society, 1998, 81, 3277-3284.	1.9	143
174	Correlation between Surface Texture and Chemical Composition in Undoped, Hard, and Soft Piezoelectric PZT Ceramics. Journal of the American Ceramic Society, 1998, 81, 721-724.	1.9	57
175	Transient Growth Bands in Silicon Nitride Cooled in Rareâ€Earthâ€Based Glass. Journal of the American Ceramic Society, 1997, 80, 1397-1404.	1.9	19
176	Thermodynamic Analysis of Grain Aspect Ratio in Fibrous Microstructures of Silicon Nitride. Journal of the American Ceramic Society, 1997, 80, 3250-3252.	1.9	8
177	Model experiments concerning abnormal grain growth in silicon nitride. Journal of the European Ceramic Society, 1996, 16, 3-14.	2.8	104
178	Short-Range and Medium-Range Order in Lithium Silicate Glasses, Part II: Simulation of the Structure by the Reverse Monte Carlo Method. Journal of the American Ceramic Society, 1996, 79, 2839-2846.	1.9	19
179	Densification Behavior and Properties of Y2O3-Containing alpha-SiAlON-Based Composites. Journal of the American Ceramic Society, 1996, 79, 1537-1545.	1.9	26
180	Short-Range and Medium-Range Order in Lithium Silicate Glasses, Part I: Diffraction Experiments and Results. Journal of the American Ceramic Society, 1996, 79, 2833-2838.	1.9	50

#	Article	IF	CITATIONS
181	Grain Boundary Films in Rareâ€Earthâ€Glassâ€Based Silicon Nitride. Journal of the American Ceramic Society, 1996, 79, 788-792.	1.9	142
182	Grain Growth Studies of Silicon Nitride Dispersed in an Oxynitride Glass. Journal of the American Ceramic Society, 1993, 76, 2778-2784.	1.9	123
183	Sintering of in-Situ Synthesized Sic-TiB2 Composites with Improved Fracture Toughness. Journal of the American Ceramic Society, 1992, 75, 2479-2483.	1.9	85
184	Slip Casting of SiC-Whisker-Reinforced Si3N4. Journal of the American Ceramic Society, 1989, 72, 765-769.	1.9	66
185	Thermodynamic Calculations for the Formation of SiC-Whisker-Reinforced Si <sub>3</sub> N <sub>4</sub> Ceramics. Advanced Ceramic Materials, 1988, 3, 557-562.	2.3	48
186	Process Development for the Ceramic Injection Molding of Oxide Chopped Fiber Reinforced Aluminum Oxide. Key Engineering Materials, 0, 742, 231-237.	0.4	4
187	Ag-Migration in La-doped PZT-Multilayers. , 0, , 446-451.		0
188	Ferroelectric domains in methylammonium lead iodide perovskite solar cells. , 0, , .		0
189	Ferroelectric domains in methylammonium lead iodide perovskite solar cells. , 0, , .		0
190	Field Assisted Sintering of Nbâ€Al <sub>2</sub> O <sub>3</sub> Composite Materials and Investigation of Electrical Conductivity. Advanced Engineering Materials, 0, , .	1.6	5